

Mini Review

Review of poly (methyl methacrylate) based polymer electrolytes in solid-state supercapacitors

Famiza Abdul Latif¹, Nabilah Akemal Muhd Zailani^{2,*}, Zeyana Saif Mubarak Al Shukaili^{1,3}, Sharil Fadli Mohamad Zamri¹, Noor Azilah Mohd Kasim⁴, Mohd Saiful Asmal Rani^{5,*}, Mohd Nor Faiz Norrrahim^{6,*}

¹ Faculty of Applied Sciences, Universiti Teknologi MARA, UiTM, Shah Alam 40450, Selangor, Malaysia

² Faculty of Applied Sciences Universiti Teknologi MARA Perlis Branch Arau Campus 02600 Arau Perlis, Malaysia

³ Ministry of education, Muscat, Sultanat Oman

⁴ Department of Chemistry and Biology, Universiti Pertahanan Nasional Malaysia, Kem Perdana Sungai Besi, 57000 Kuala Lumpur, Malaysia

⁵ School of Materials and Mineral Resources Engineering, Engineering Campus, Universiti Sains Malaysia, 14300 Nibong Tebal, Penang, Malaysia

⁶ Research Centre for Chemical Defence, Universiti Pertahanan Nasional Malaysia, Kem Perdana Sungai Besi, 57000 Kuala Lumpur, Malaysia

*E-mail: nabilahakemal@uitm.edu.my, iker.asmal55@gmail.com, faiznorrrahim@gmail.com

Received: 18 August 2021 / Accepted: 13 November 2021 / Published: 6 December 2021

Solid polymer electrolytes (SPEs) have been used as a promising electrolyte for supercapacitors due to their high processing flexibility and electrode–electrolyte interaction. Poly (methyl methacrylate) (PMMA)-based SPEs have received considerable interest due to their ease of synthesis, low mass density, strong mechanical stability, low binding energy with ionic salts, and excellent charge carrier mobility. In order to overcome the low room-temperature ionic conductivity and poor thermodynamic stability in high-voltage devices (> 4.2 V) of the PMMA materials, composition modulations incorporating PMMA with ionic liquids have been designed, which could effectively enable the applications of PMMA-based SPEs with widened electro-stable voltage ranges. In this review, we explain the fundamental physical properties of PMMA as a suitable polymer host in SPEs, as well as numerous modifications to overcome its brittleness. Some explanation of the types of polymerisation reactions is discussed and the free radical polymerisation of methyl methacrylate in ionic liquid is specifically reviewed. Further advancements and enhancements to PMMA-based materials for building of improved supercapacitors were also revealed.

Keywords: solid-state polymer electrolytes; poly (methyl methacrylate); supercapacitors; ionic conductivity; electrochemical stability.

1. INTRODUCTION

In the 21st century, nobody can envision a world that has revolutionised our lifestyles and made us feel more comfortable without portable/wearable electronic equipment, i.e., mobile phones, laptop computers, cameras, smartwatches, activity monitoring gadgets, etc. Improved energy storage systems are required to increase the energy consumption of such intelligent devices. In fact, electrochemical energy storage is becoming increasingly vital as we build a sustainable post-fossil fuels era. Supercapacitors and batteries are the most successful players on the Ragone chessboard, with extensive research in both academia and industry [1-4]. Supercapacitors and batteries are distinguished primarily by their charge storage mechanisms and materials/structures. Batteries normally give high energy density by storing charge in bulk electrodes via faradaic reactions, whereas supercapacitors can provide high power density due to surface charge storing mechanisms [5, 6]. The Ragone plot illustrates the P (specific power) vs. E (specific energy) curve for several energy storage devices (Figure 1). Capacitors have a very high specific power capability but a very low specific energy. In contrast, despite their high specific energy, batteries and fuel cells have poor power delivery or uptake. The desire to establish a new way for producing faster and more powerful energy storage systems led to the discovery and development of supercapacitors, which can bridge the gap between the batteries/fuel cells and conventional capacitors [6, 7].

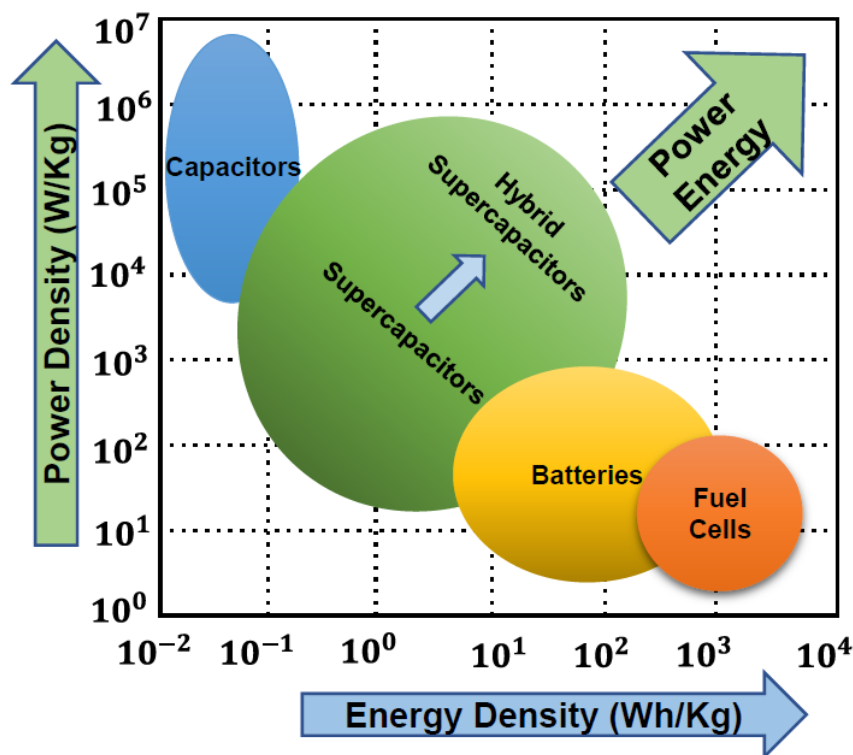


Figure 1. Specific power vs. specific energy (Ragone Plot) for various energy storage devices. Reproduced with permission from ref [8].

Aside from the cycle-life (or lifetime), the energy density and power density are the two most important properties to consider when evaluating electrochemical energy systems. In Ragone plots, supercapacitors are located between conventional dielectric capacitors and batteries/fuel cells [9]. Despite having a significantly lower energy density than batteries or fuel cells, electrochemical supercapacitors can have substantially higher power densities. As a result, they appear to be promising for use in current stabilisation when gaining access to intermittent renewable energy sources. Furthermore, electrochemical supercapacitors have sparked the interest of a wide range of applications that require high power density, including portable electronics, electric or hybrid electric vehicles, aircraft, and smart grids. For instance, electrochemical capacitors could provide a high-power density for short-term acceleration and energy recovery during braking in hybrid and electrical vehicles, including fuel cells, thereby saving energy and protecting batteries from high-frequency rapid discharge and charging process (dynamic operation).

However, when compared to batteries and fuel cells, the main disadvantage of electrochemical supercapacitors is their low energy density i.e. electrical double layer capacitors (EDLC) typically have an energy density of less than 10 W h kg^{-1} ; even pseudocapacitors and hybridcapacitors have energy densities of less than 50 W h kg^{-1} , which cannot fully meet the growing demand of applications requiring high energy densities [10]. Considerable work has been expanded in boosting the energy density of electrochemical supercapacitors to widen their application possibilities. In the development of electrochemical supercapacitor electrolytes, expanding the potential window of an electrolyte solution, i.e. increasing the cell voltage (V), can efficiently boost the energy density. In terms of improving energy density, increasing cell voltage is more efficient than increasing electrode capacitance. This is owing to the fact that energy density is proportional to the square of cell voltage. As a result, creating novel electrolytes/solutions with broad potential windows should take precedence over inventing new electrode materials.

The ideal electrolyte must have the following characteristics: (i) a broad-potential screen; (ii) high ion conductivity; (iii) high chemical and electrochemical stability; (iv) high chemical and electrochemical supercapacitor inertness componential (i.e., the electrodes, current collectors and packaging). Actually, all of these conditions are extremely difficult for an electrolyte to meet, and each electrolyte has its unique set of advantages and deficiencies. In the first section of this paper, the main performance metrics and the relationship between electrochemical supercapacitors and electrolytes are presented. The next section provides a comprehensive overview of poly (methyl methacrylate) (PMMA) properties and the electrical system based on PMMA. In order to understand the performance impacting factors of electrolyte design and optimization, electrolyte effects in the electrochemical supercapacitor performance are addressed. The final section covers the major research and development challenges and perspectives in electrochemical supercapacitor electrolyte research, as well as potential research directions to help to overcome challenges.

2. PROPERTIES OF POLY (METHYL METHACRYLATE)

The solid polymer electrolytes (SPE) were reported to replace liquid electrolytes over four decades ago, in 1973, due to their superior mechanical, thermal, and ionic conductivity capabilities. It has proposed a solution to the challenges encountered by liquid electrolytes, i.e. leakage, electrode reaction, and poor chemical stability [11, 12]. Many investigations have been carried out to develop solid polymer electrolytes from diverse materials such as polyethylene oxide, polyacrylic acid, and polyvinyl alcohols have been widely used as host polymers [13-15].

PMMA is a synthetic polymer derived from the monomer methyl methacrylate. Its IUPAC designations are poly [1-(methoxy carbonyl)- 1-methyl ethylene] from a hydrocarbon standpoint and poly (methyl 2-methylpropenoate) from an ester standpoint. PMMA was discovered by British scientists Rowland Hill and John Crawford in the early 1930s. It was first used by a German scientist, Otto Rohm in 1934. PMMA is a clear, colourless polymer with a glass transition temperature range of 100 °C to 130 °C, and a density of 1.20 g cm³ at room temperature [16].

This transparent thermoplastic is commonly utilised as a substitute for inorganic glass because of its lightweight, shatter-resistant, high impact strength and favourable processing conditions. PMMA is a promising polymer for use in polymer electrolytes, drug delivery systems, optical devices and also for biomedical applications. PMMA is discovered to be an amorphous thermoplastic due to the presence of the adjacent methyl group (CH₃) in the polymer structure which prevents it from packing tightly in a crystalline way (Figure 2) [16]. The oxygen atoms in PMMA (C=O and –OCH₃ groups) will form coordination bonds with the cations from the IL or the doping salt. Thus, PMMA has met the requirements for a suitable polymer host in electrolyte system.

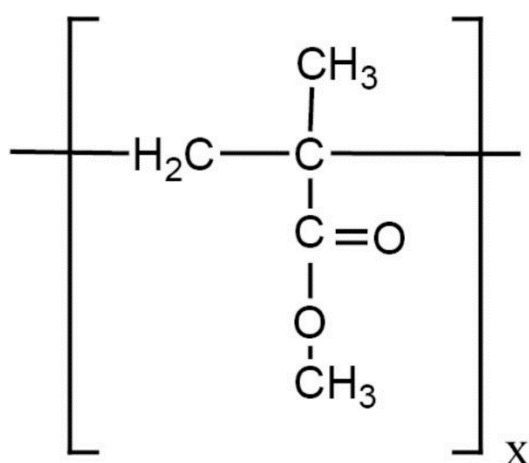


Figure 2. PMMA structure.

PMMA is widely employed as a polymer host in polymer electrolytes systems due to its lithium electrode stability (Table 1) [17]. The stability towards lithium electrode can only be achieved when PMMA is fabricated in thin film form. To date, fabricating PMMA film has been difficult because

commercial PMMAs create brittle films that do not stick well to the electrode, providing additional resistance (the air gap) for ionic conduction [18, 19].

Thus, several modifications have been made to improve the interface between the electrode and the electrolyte, i.e. blending it with another polymer [20, 21], adding plasticizers [22, 23], copolymerization [11] or organic fillers [24, 25], etc. These attempts were mostly unsuccessful due to poor mechanical properties induced by the higher amount of plasticizer, agglomeration caused by the filler and poor film homogeneity when blended with other polymers.

Ionic liquids (IL) such as 1-butyl-3-methylimidazolium bis(trifluoromethylsulfonyl) imide [26], 1-butyl-3-methylimidazolium tetrachloroferrate [27] have recently been used to improve the brittleness of the film. However, the ionic conductivities achieved were still poor, i.e. less than 10^{-4} S cm⁻¹ which is below the minimum requirement for use in any electrochemical device [28]. This is most likely owing to the polar nature of PMMA, which is prone to interchain crosslinking via hydrogen bonding, reducing the flexibility of the polymer chain [29]. As a result, research into producing a new type of PMMA with the ability to make flexible SPE films is critical to reap the benefits of this polymer as polymer electrolytes.

Table 1. Some examples of PMMA electrolyte systems

System	Conductivity (30 °C, S cm ⁻¹)	References
PMMA/LiClO ₄	6.07×10^{-9}	[30]
PMMA/LiCF ₃ SO ₃	9.88×10^{-5}	[31]
PMMA/Li ₂ SO ₄ /DBP	3.43×10^{-6}	[32]
PMMA/LiTf/ PC	6.46×10^{-6}	[33]
PMMA/LiBF ₄ /EC-PC	2.24×10^{-3}	[22]
PMMA/LiCF ₃ SO ₃ /SiO ₂	5.63×10^{-7}	[34]
PMMA/LiCF ₃ SO ₃ /EC/SiO ₂	2.15×10^{-5}	[35]
PMMA/PEO/LiTFSI/Al ₂ O ₃	9.39×10^{-7}	[20]
PMMA/ENR-50/LiCF ₃ SO ₃	5.09×10^{-5}	[18]
PMMA/ENR-50/LiBF ₄ /D-SiO ₂	5.06×10^{-7}	[24]
PMMA/PVC/ BmimTFSI	1.64×10^{-4}	[19]
PMMA/PVdF/AgNO ₃	9.13×10^{-4}	[36]
PVDF-HFP/PMMA/LiClO ₄ /DEC-PC	3.97×10^{-4}	[37]
PMMA/LiTFSI/TEGDME	2.8×10^{-3}	[38]
PEO-PS-PMMA/LiPF ₆ /EC-DMC	0.12×10^{-3}	[39]

3. IONIC LIQUIDS BASED ELECTROCHEMICAL SUPERCAPACITOR ELECTROLYTES

The IL or also known as molten salts can be defined as organic salts which remain in liquid form at room temperature.

Table 2. Ionic liquids as solvents for organic and catalytic reactions

Type of ionic liquid	Reactions	References
<u>Organic reaction</u>		
(i) 1-butyl- 3-methylimidazolium hexafluorophosphate [BMI][PF ₆]	Nucleophilic displacement: Cl → CN	[40]
(ii) 1-butyl- 3-methylimidazolium tetrafluoroborate [BMI][BF ₄]	Wittig reaction	[41]
<u>Catalysed reaction</u>		
(i) 1-butyl- 3-methylimidazolium tetrafluoroborate [BMI][BF ₄]	Allylic alkylation Catalyst: Pd(OAc) ₂ /phosphine	[42]
(ii) 1-butyl- 3-methylimidazolium hexafluorophosphate [BMI][PF ₆]	Coupling of aryl halide Catalyst: [(PPh ₃) _n Ni(0)]	[43]

They are made up of bulky organic cations and small inorganic or organic anions [19, 44]. IL are getting considerable interests from academics and industrialists as an alternative to traditional organic solvents due to its unique combinations of low volatility, chemical stability, ability to dissolve organic and inorganic solutes/gases and tunable solvent properties [45]. In addition, the low volatility of IL can contribute to “green chemistry” by reducing emissions of harmful volatile organic compounds. Thus, over the last few years, IL have been widely used as solvents in organic and catalytic reactions (Table 2).

IL also has excellent ionic conductivity and a wide range of electrochemical media, making them appropriate for use as electrolytes in electrochemical devices [45, 46]. A few applications of IL as electrolytes were tabulated in Table 3.

Table 3. Ionic liquids as electrolytes in electrochemical devices.

Type of ionic liquid	Application	References
(i) N, N-diethyl-N-methyl-N-(2-methoxyethyl) ammonium tetrafluoroborate [DEME][BF ₄]	Electrical double layer capacitors	[47]
(i) 1-ethyl-3-methylimidazolium bis(trifluoromethylsulfonyl) imide [EMIM][TFSI]/ Lithium bis(trifluoromethylsulfonyl) imide (LiTFSI)	Lithium batteries	[48]
(ii) 1,2-dimethyl-3-propylimidazolium bis (trifluoromethylsulfonyl)imide [DMPIM][TFSI]/ Lithium bis(trifluoromethylsulfonyl) imide (LiTFSI)		
(i) 1-propyl-3-methylimidazolium iodide [PMIM][I]	Dye-sensitized solar cells	[49]
(ii) 1-ethyl-3-methylimidazolium thiocyanate [EMIM][TCN]		

3.1. Immobilisation of ionic liquids into PMMA

Although the IL are deemed as suitable for electrolyte purposes, yet their applications are limited due to their liquid nature at room temperature which are susceptible to leakage problem. Thus, it is advantageous for the IL to be immobilised in the polymer. There are three methods to immobilise the IL in the PMMA polymer matrix including:

3.1.1. Doping of ionic liquids into the PMMA polymer matrix

Various types of IL have been doped or added into the polymer matrix using solution casting method. It was observed that the ionic conductivities obtained for these IL-doped polymer systems are higher if compared to their neat polymer. Thus, it can be said that, despite being the source of mobile ion, IL also acts as a plasticiser which increases the amorphous content of the polymer electrolytes hence contributing to the enhancement of the ionic conductivity [50]. Table 4 lists the ionic liquid as dopant in PMMA-based polymer electrolyte system. The proper choice of the ionic liquid and polymer is also important in obtaining the optimum value of conductivity.

Table 4. Ionic liquid as dopant in PMMA-based polymer electrolyte systems

Polymer/IL	Ionic conductivity (30 °C, S cm ⁻¹)	Properties	References
PMMA/DMOImTf	1.92×10^{-6}	-	[51]
PMMA/[BMIM][TFSI]	7.8×10^{-4}	- Produced highly stretchable film with at least four-fold stretchability	[52]
PMMA/[BMIM] [FeCl ₄]	$\sim 10^{-5}$	- Produced transparent and flexible ionogel film	[27]
PMMA/PtEu ₂ /[BMIM][NTf ₂]	$\sim 10^{-6}$	- Produced transparent and flexible ionogel film	[26]
PVDF-HFP/PMMA-[BMIM]BF ₄	1.4×10^{-3}	-	[53]
PMMA-PUA - DEEYTFSI-LiTFSI	2.76×10^{-4}	- Electrolyte has stable compatibility with LiFePO ₄ cathode	[54]

3.1.2 The polymerisation of polymerisable ionic liquids

The polymeric IL is obtained by polymerising the IL after introducing vinyl group into its cationic or (and) anionic structure. The radical polymerisation of the IL monomers produces a polymer chain in which anion, or the cation of IL is attached to the polymer backbone, hence creating a single ion-conducting IL polymer.

Table 5. Some examples of polymeric ionic liquids

Type of polymeric ionic liquids	Ionic conductivity (S cm ⁻¹)	Properties	References
Poly 1-vinyl-3-ethylimidazolium bis (trifluoromethanesulfonyl) imide	7.65×10^{-8} (20 °C)	Transparent and solid films	[55]
Poly (diallyldimethylammonium) bis (trifluoromethanesulfonyl) imide /LiTFSI	6.48×10^{-6} (23 °C)	Free-standing and transparent films, but became rigid and fragile at high salt content	[56]

The covalent bonding of this component ions (anion or cation) with the vinyl group suppresses the mobility of the ions and also gives rise to the T_g of the polymer. This explains the lower ionic conductivity of the polymeric IL if compared to the pristine IL [57]. 5 lists the polymeric IL obtained in the previous studies.

3.1.3. The polymerisation of a vinyl monomer in IL

As a large number of vinyl monomers are soluble in IL, the polymerisation of various monomers in the presence of IL is carried out in order to have control over the physical and chemical nature of the polymer obtained. However, not all monomers are compatible with the IL. The polymer electrolytes obtained from compatible polymers in chloroaluminate molten salts have been reported to possess high ionic conductivity. However, they are not suitable for applications due to their high sensitivity to moisture [58]. Then, the report on air and water stable non-chloroaluminate IL such as 1-ethyl-3-methylimidazolium has generated renewed interest in these materials [59].

Noda and Watanabe (2000) had reported on the in situ free radical polymerisations of vinyl monomers (e.g.: methyl methacrylate, acrylonitrile, vinyl acetate, styrene, 2-hydroxymethyl methacrylate) in 1-ethyl-3-methylimidazolium tetrafluoroborate (EMIBF₄) and 1-butylpyridinium tetrafluoroborate (BPBF₄) [60]. The mixture of vinyl monomer and IL were heated at 80 °C for 12 h in the presence of 0.5 wt % benzoyl peroxide (BPO) as an initiator. Table 6 shows the compatibility of EMIBF₄ and BPBF₄ with MMA. It was reported that the poly (2-hydroxyethyl methacrylate) (PHEMA) showed good compatibility with BPBF₄ and gave transparent, mechanically strong and highly conductive polymer gels with ionic conductivity of 10^{-3} S cm⁻¹ (HEMA: IL; 4:6) at ambient temperature.

Table 6. Compatibility studies of some IL in the polymerisation of MMA

Type of Monomers	EMIBF ₄ [60]		BPBF ₄ [60]		EMITFSI [61]		BMIPF ₆ [62]	
	M	P	M	P	M	P	M	P
Methyl methacrylate	X	-	√	X	√	√	√	√

M: monomer, P: polymer obtained, √: compatible, X: not compatible, O: no polymerisation

In situ free radical polymerisations of vinyl monomers (e.g.: methyl methacrylate, acrylonitrile, vinyl acetate, styrene, 2-hydroxymethyl methacrylate, methyl acrylate, acrylamide) in 1-ethyl-3-methylimidazolium bis(trifluoromethane sulfonyl)imide (EMITFSI) were also investigated [61]. The IL and monomer were mixed, and the polymerisation took place at 80 °C for 12 h in the presence of 2 mol% BPO. The compatibility of EMITFSI with monomers and their polymers presented (Table 6). It was revealed that PMMA was compatible with EMITFSI, and it was possible to develop self-standing, flexible, and translucent polymer gels with ionic conductivity of 10⁻² S cm⁻¹.

Investigation on the preparation of gel polymer electrolytes by in situ free radical polymerisation of vinyl monomers (e.g.: methyl methacrylate, acrylonitrile, vinyl acetate, styrene and acrylamide) in 1-butyl-3-methylimidazolium hexafluorophosphate (BMIPF₆) was explored [62]. The polymerisation was carried out by heating the monomer-BMIPF₆ mixture at 80 °C for 12 h in the presence of 1 wt% azobisisobutyronitrile (AIBN) as an initiator. When 40 wt% of IL was added, the results showed that PMMA has good compatibility with BMIPF₆, and a gel polymer film with a high ionic conductivity of ~10⁻³ S cm⁻¹ was achieved. It may be inferred that IL compatibility with the monomer or polymer is critical in the designing of a new polymer by free radical polymerisation of vinyl monomer in IL.

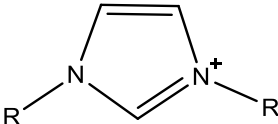
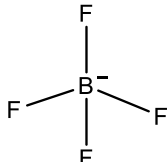
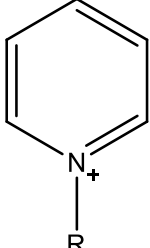
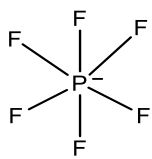
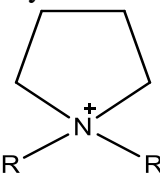
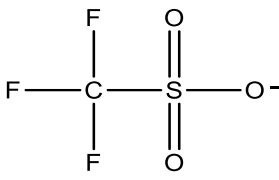
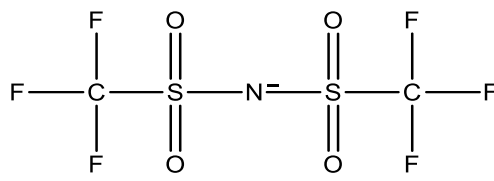
3.2. The commonly used cations and anions of ionic liquids in polymer electrolyte systems

The most often employed cations and anions in PE systems for IL was presented (Table 7). 1-alkyl-3-methylimidazolium cations are the most commonly utilised in ILs [44, 45] as they are easy to handle, stable against water and have high ionic conductivity [59, 63]. The physical properties of the imidazolium IL such as melting point, density, viscosity, hydrophobicity and miscibility with other solvents can be customized only by modifying the type and/or position of the substituents at the imidazolium cation [45], i.e., increasing the alkyl chain length from butyl to octyl of 1-alkyl-3-methylimidazolium cations increases the hydrophobicity and viscosity of IL while decreasing densities and surface tension values [44]. The characteristics of the IL may also vary depending on the type of the anion. It has been established that the viscosity of the 1-alkyl-3-methylimidazolium IL decreases as paired with the anion of Cl⁻ > PF₆⁻ > BF₄⁻ ≈ NO₃⁻ > NTf₂⁻.

The anion which is of particular interest nowadays is the trifluoromethylsulfonylimide [NTf₂]⁻ anion that gives particularly thermally stable salts (up to 400 °C) [44]. The [NTf₂]⁻ anion has a diffuse charge that can be explained by the delocalisation of charge from the nitrogen onto the neighbouring sulphur atom which subsequently results in a little delocalisation onto oxygens. The strength of the ion-

ion interaction with the neighbouring cation was reduced in order to shield the delocalised charge. As a result of its reduced interaction with cation, this imide anion is likely to be more mobile than triflate anion.

Table 7. The commonly used cations and anions of IL.

Cations	Anions
 <p>Imidazolium</p>	 <p>Tetrafluoroborate</p>
 <p>Pyridinium</p>	 <p>Hexafluorophosphate</p>
 <p>Pyrrolidinium</p>	 <p>Triflate</p>
	 <p>Bis (trifluoromethylsulfonyl) imide</p>
	<p>Br⁻ Bromide Cl⁻ Chloride</p>

The IL, 1-methyl-3-pentamethyldisiloxymethylimidazolium bis(trifluoromethylsulfonyl)imide, $[(\text{SiOSi})\text{C}_1\text{C}_1\text{im}][\text{NTf}_2]$ was commonly used in free radical polymerisation of MMA (Table 8) [64]. The bulky structure of $[(\text{SiOSi})\text{C}_1\text{C}_1\text{im}][\text{NTf}_2]$ is expected to prevent hydrogen bonding in the PMMA chain, resulting in flexible films. This IL has a high ionic conductivity of $\sim 10^{-3} \text{ S cm}^{-1}$, which could be attributed to negative charge delocalisation $[\text{NTf}_2]^-$. Aside from that, the bulky structure of imidazolium

cation, $[(\text{SiOSi})\text{C}_1\text{C}_1\text{im}]^+$ and the delocalisation of the charge over N-C-N moiety in the ring both contribute to the decrease in ion-ion interaction.

Table 8. Properties of $[(\text{SiOSi})\text{C}_1\text{C}_1\text{im}] [\text{NTf}_2]$

Properties of $[(\text{SiOSi})\text{C}_1\text{C}_1\text{im}] [\text{NTf}_2]$	
Conductivity	$1.14 \times 10^{-3} \text{ S cm}^{-1}$
Viscosity	89 mPa.s (293K)
Density	1.32 g cm^{-3}
Molecular weight	$523.62 \text{ g mol}^{-1}$

4. SALT AS THE DOPANT IN POLYMER ELECTROLYTE SYSTEMS

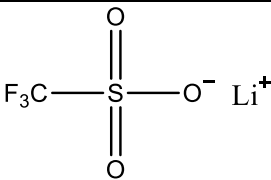
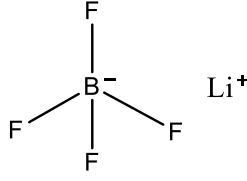
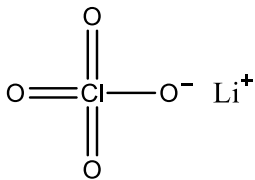
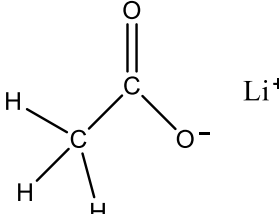
Polymers are recognized to be electrical insulators in general. By incorporating a few ions from inorganic salt into the polymer host structure to produce polymer-salt complexes, i.e., polymer electrolytes, these materials can be converted into conducting materials. In the 1970s, Fenton and Wright were the first to investigate polymer electrolytes [65, 66]. Poly (ethylene oxide) (PEO) mixed with alkali metal salts was discovered to be the first ion conducting polymer. Armand et al. (1979) discovered the solid-state battery utilizing PEO-Li salt, which was the first conceivable application of polymer electrolytes [67]. Since then, numerous polymer electrolytes containing various mobile ions such as NH_4^+ , Li^+ , Na^+ , K^+ , Ag^+ , Cu^+ , Mg^{2+} , and others have been reported in the literature. It has gained increasing interest in practical applications due to a variety of important features such as ease of fabrication, flexibility, good electrode-electrolyte interaction, cost effectiveness, and mechanical stability [68].

The recent development of solid polymer electrolytes based on biopolymer materials has yielded promising results. These materials were utilized to create biopolymer electrolyte films by including acids or salts. Proton carriers have included strong acids such as phosphoric acid (H_3PO_4) and sulfuric acid (H_2SO_4). They do, however, damage biopolymers, making them unsuitable for practical use [69]. Alternatively, many compounds, such as lithium iodide, potassium iodide, ammonium thiocyanate, ammonium chloride, sodium iodide, ammonium nitrate, magnesium acetate, and others, were used to make solid electrolytes [12, 23, 70, 71]. Polymer electrolytes have been extensively investigated due to their conductive qualities for prospective applications in electrochemical devices such as lithium, sodium, and proton batteries [1, 72, 73], dye-sensitized solar cells [11, 13], and supercapacitors [62, 74]. The size of the salt cation determines the ionic conductivity of polymer-based electrolytes.

An organic salt consists of a positively charged cation and negatively charged anion. The commonly used cations in PE systems are Li^+ , Mg^{2+} and Na^+ while anions such as CF_3SO_3^- , CH_3COO^- , BF_4^- and I^- are widely used. The lithium-ion based salt is most preferred due to the small size of lithium ion (0.76 \AA) if compared to sodium ion (1.06 \AA) and this facilitates the mobility of the ions across the medium in polymer electrolytes. The lattice energy of the salts must be overcome to allow the dissociation of the salt. Thus, salts of large anions such as ClO_4^- , BF_4^- , CF_3SO_3^- and CH_3COO^- are more

preferred as they own low lattice energy which ease the dissociation of the salt hence providing more free ions for ionic conduction. The lattice energies for the lithium-ion based salts (Table 10) [75].

Table 10. Lattice energies of some lithium-ion based salts

Salt	Lattice energy, U (kJ mol ⁻¹)
	Lithium triflate (LiTf) 725
	Lithium tetrafluoroborate (LiBF ₄) 699
	Lithium iodide (LiI) 757
	Lithium perchlorate (LiClO ₄) 723
	Lithium acetate (LiAc) 881

LiTf is one of the ionic salts that usually added to the newly synthesised PMMA to provide additional conducting species to gain higher ionic conductivity. Aside from its large size of the anion, LiTf owns a highly delocalised structure which contributes to its low lattice energy. The delocalisation of the negative charge occurs at the anion via electron withdrawing group of $-CF_3$ which reduces the electrostatic attraction between the cation and anion [76]. However, the addition of a high amount of salt and low dielectric constants of solvents contribute to the formation of ion pairs and ionic aggregates which reduce the ionic conductivity of the polymer electrolytes [58].

5. POTENTIAL OF PMMA BASED POLYMER ELECTROLYTES AS ELECTROCHEMICAL SUPERCAPACITORS

Nowadays, the need for energy is increasing due to the rapid growth of the global population and economy. However, due to global warming and resource depletion concerns the use of traditional fossil fuels as energy sources is a subject of concern. Renewable energies (e.g., solar, wind and tidal energy)

were created at the time, however these sources are heavily reliant on the natural environment. Thus, the best alternative is an energy storage device that is extremely efficient, stable, and environmentally benign. Batteries, supercapacitors and fuel cells are the most commonly utilized energy storage devices [68, 77]. The performance of these devices depends on how much charge can be stored and how quickly the charge can be stored and released. Therefore, the energy density (E) (Equation (1)) and power density (P) (Equation (2)) of these energy storage devices are two important parameters in evaluating their performances.

$$E = \frac{CV^2}{2} \tag{1}$$

$$P = \frac{V^2}{4R_s} \tag{2}$$

where C equals to specific capacitance, V equals to voltage and R_s denotes to equivalent series resistance. Thus, to get high values of E and P , C and V need to be increased while reducing R_s .

Supercapacitors can be divided into three categories including EDLC, pseudocapacitors and hybrid capacitors (Table 11).

Table 11. Characteristics for different types of supercapacitors [78]

	EDLC	Pseudocapacitors	Hybrid capacitors
Charge storage	Electrostatically (Helmholtz layer)	Electrochemically (Faradaic charge transfer)	Electrostatically and electrochemically
Types of electrodes	- Activated carbons - Carbon aerogels - Carbon nanotubes	- Conducting polymers - Metal oxide	- Composite hybrids - Asymmetric hybrids - Battery-type hybrids
Capacitance	Lower capacitance if compared to pseudocapacitors and hybrid capacitors	High capacitance	High capacitance
Lifetime	Longer lifetimes	Shorter lifetime	Shorter lifetime

The advantage for each type of supercapacitors is determined by how they store energy. As the EDLC stores energy electrostatically, so there is no faradic reaction at the electrodes, which minimises swelling in the active material that can occur to pseudocapacitors and hybrid capacitors during the

charge-discharge cycle. This can be attributed to EDLC having a longer lifetime than the other two types of supercapacitors [78, 79].

There are several types of carbon used as electrodes in EDLC, with activated carbons (ACs) being the most prevalent due to their high surface area (1000-2000 m²/g), low cost, high conductivity and good chemical stability [80]. When ACs are used as electrodes in EDLC, cost-effective applications with longer lifetime can be designed.

5.1. Evaluation on PMMA based polymer electrolytes in EDLC

A few characterization parameters, such as electrochemical impedance spectroscopy (EIS), linear sweep voltammetry (LSV), cyclic voltammetry (CV) and charge-discharge (CD) test can be used to evaluate the performance of EDLC. The LSV test is used to determine the stable operational voltage range as well as the decomposition voltage of the EDLC cell. This test must be performed before to any other characterisations so that a suitable range of voltage may be applied in CV and CD measurements to avoid electrolyte damage throughout the tests. For non-aqueous (organic and ionic liquid) electrolytes, the working voltage of a symmetric EDLC cell is in the range of 2-3 V [81]. Among the factors that may influence the operational stability window of the cell are: (a) dielectric constant, ϵ_r of the polymer and (b) lattice energy of the salt [82].

5.1.1. Electrochemical impedance spectroscopy

Electrochemical impedance spectroscopy (EIS) is used to determine the electrical properties of a material. This method involves the application of a fixed voltage across two identical electronically conducting electrodes of a sample holder that are in contact with the sample at different frequencies. The Nyquist plot, also known as the impedance plot have been shown to be particularly useful in determining impedance parameters [83, 84]. The bulk resistance (R_b) of each sample is determined from the Nyquist plot obtained, and hence the conductivity (σ) of the sample is calculated using Equation

$$\sigma = \frac{l}{R_b \cdot A} \quad (3)$$

where R_b is the bulk resistance (Ω), l is the thickness of the film (cm) and A is the effective electrode and the electrolyte contact area (cm²). A micrometre screw gauge is used to measure the thickness of the samples.

Dielectric studies can be performed using impedance data to get a better understanding of the ionic transport behaviour of polymer electrolyte systems. The dielectric constant (ϵ_r) can be defined as the measure of the stored electric charge whereas the dielectric loss (ϵ_i) is the measure of the energy dissipated to align the charge in each cycle of the applied electric field [85]. The real part of electrical modulus (M_r) and imaginary electric modulus (M_i) are the reciprocal of the ϵ_r and ϵ_i respectively [86, 87]. The following equations can be used to calculate the values of ϵ_r , ϵ_i , M_r and M_i :

$$\varepsilon_r = \frac{Z_i}{\omega \cdot C_0 (Z_r^2 + Z_i^2)} \quad (4)$$

$$\varepsilon_i = \frac{Z_r}{\omega \cdot C_0 (Z_r^2 + Z_i^2)} \quad (5)$$

$$M_r = \frac{\varepsilon_r}{(\varepsilon_r + \varepsilon_i)} \quad (6)$$

$$M_i = \frac{\varepsilon_i}{(\varepsilon_r + \varepsilon_i)} \quad (7)$$

where C_0 is equal to $\varepsilon_0 A/t$, ε_0 is the permittivity of the free space (8.85×10^{-14} F cm⁻¹) and ω is equal to $2\pi f$. By referring to the M_i obtained in Equation (7), the relaxation time can be calculated using the relation below [87]:

$$\tau_\sigma = \frac{1}{2\pi f_{\max}} \quad (8)$$

where τ_σ is the conductivity relaxation time and f_{\max} is the frequency corresponding to M_i peak.

For an ideal system, the semicircle with the centre on the x -axis and vertical spikes are expected. However, depressed, or distorted semicircles and slanted or curved spikes are observed in many real systems. The deviations from the ideal behaviour are contributed by a few factors such as non-ideal nature of capacitors, distribution of microscopic properties of the material and the unevenness of the electrode-electrolyte interfaces [87, 88].

The AC impedance spectra of polyethylene oxide (PEO)/ polymethyl methacrylate (PMMA)-ethylene carbonate (EC)-LiClO₄-silica aerogel based solid polymer electrolyte (SPE) along with their equivalent circuit model is illustrated in Figure 3 [89]. The spectra show a semicircle at high frequency (corresponds to ion migration in the bulk system) followed by a spike at low frequency (corresponds to the capacitance characteristic of the sample) [23, 90]. The equivalent circuit is made up of R_b and C_b connected in series with C_e , where R_b and C_b are the electrolyte's bulk resistance and capacitance, respectively, and C_e is the interfacial capacitance.

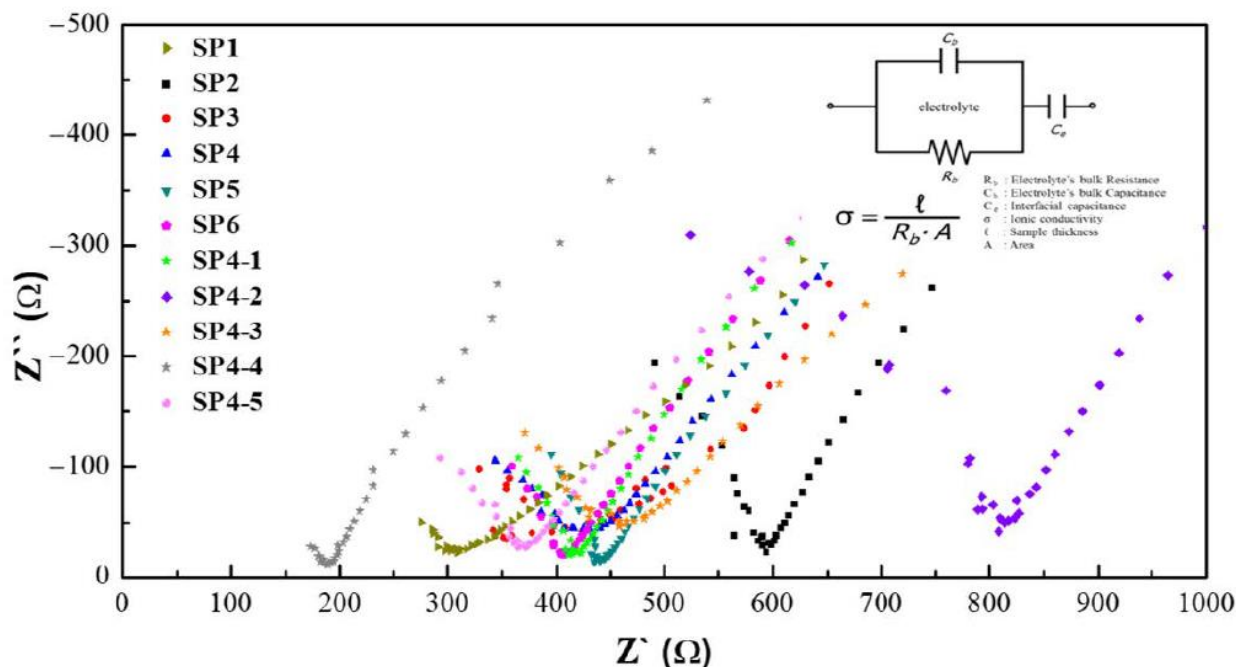


Figure 3. AC impedance spectra of PEO-PMMA-LiClO₄-silica aerogel based SPE [89].

5.1.2. Linear sweep voltammetry

Linear sweep voltammetry (LSV) was used to confirm the stability window of the polymer electrolyte. Arof and co-researchers investigated the potential application of EDLC using poly(methyl methacrylate)-C₄BO₈Li gel polymer electrolyte and carbonaceous material from shells of mata kucing (*Dimocarpus longan*) fruit which shows the stability window was 1.7 V and -1.7 V for the anodic and cathodic cycles, respectively. This finding implying that the polymer electrolyte is appropriate for EDLC applications with operating voltages up to 1.7 V since this is the region where the polymer electrolyte does not undergo any chemical transformation [91].

5.1.3. Cyclic voltammetry

The nature of charge storage in EDLC is investigated by cyclic voltammetry (CV) study and the specific capacitance (C_{sp}) also can be calculated using the equation below [92].

$$C_{sp} = \frac{i}{sm} \tag{9}$$

where i is the average anodic-cathodic current (A), s is the potential scan rate (Vs⁻¹) and m is the average mass of the electrodes (g).

Figure 4 shows the cyclic voltammograms of polyacrylonitrile/ poly(methyl methacrylate)/ enzymatically hydrolyzed lignin (PPLCNFs) were recorded at scanning rates of 10- 500 mV s⁻¹ [93]. The overall shapes of the curves were nearly rectangular and symmetric, indicating perfect capacitive behaviour and high reversibility. This is due to the PPLCNFs-0.5 g pore and cross-linked structures,

which can be used as rapid ion transport channels. In other work, the potential of ionogel based PMMA in supercapacitors has been explored [94]. The CV curves of [P14666] [NTf₂] + PMMA, [P14666] [DCA] + PMMA, and [P14666] [Cl] + PMMA based supercapacitor cells at a scan rate of 10 mV/s, exhibiting almost rectangular shape, indicating that the storage capability of cells is provided by the formation of two layers capacitance at the electrode-electrolyte interface. The absence of redox peaks in all CVs confirms that a non-faradaic reaction occurs and that EDLC is provided solely by charge accumulation at the electrode-electrolyte interface [91]. In other work, the cyclic voltammograms of EDLC cell recorded for mata kucing shell carbon/polymer electrolyte/mata kucing shell carbon at 10, 20, 50 and 100 mV s⁻¹. The EDLC CV profile at 10 and 20 mV s⁻¹ is essentially rectangular, with no apparent peaks attributable to redox reaction. The low scan rate voltammograms had nearly perfect horizontal plateaus, showing that ion diffusion occurs at a fairly consistent rate with little influence from ohmic resistance [95]. As the scan rate rose, the effect of equivalent series resistance (ESR) could be seen. When the potential sweep is reversed, the current takes longer to attain a constant value. At higher scan speeds, the latency is longer. The EDLC is affected by the scan rate, which is typical of capacitor cells [96].

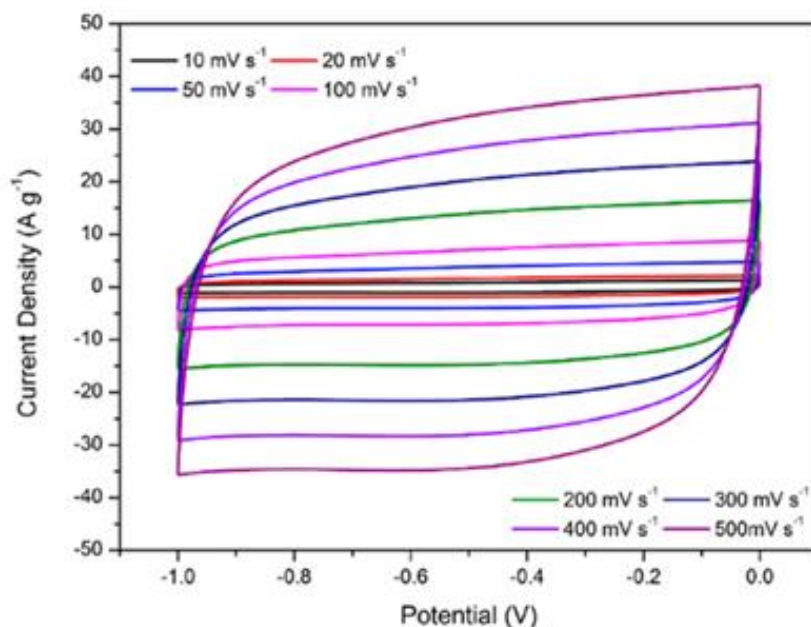


Figure 4. CV plots of PPLCNFs-0.5 g measured at 0.5- 10 Ag⁻¹ [93].

5.1.4. Charge discharge

The charge-discharge (CD) study is done to inspect the electrochemical property of EDLC upon the charge and discharge processes. The information regarding the specific capacitance (C_{sp}), cycle stability, power density (P), energy density (E) and Coulombic efficiency (η) of the assembled cell can be obtained using equations below [80, 97].

$$C_{sp} = \frac{I}{m \left(\frac{dV}{dt} \right)} \quad (10)$$

$$E = \frac{C_{sp} \times (dV)^2}{2} \times \frac{1000}{3600} \quad (11)$$

$$P = \frac{I \times dV}{2 \times m} \times 1000 \quad (12)$$

$$\eta = \frac{t_d}{t_c} \times 100 \quad (13)$$

where I is the applied current (A), m is the average mass of the electrodes, dV represents the potential change of a discharging process excluding the internal resistance drop occurring at the beginning of the cell discharge, and dt is the time interval of the discharging process. The dV/dt is determined from the slope of the discharge curve. t_d and t_c are the discharging and charging time respectively.

The charging and discharging process in EDLC was shown in Figure 5. When an external voltage is applied to the EDLC cell, the electron from one of the carbon electrodes transfers from a positive electrode to the negative electrode. The poles that the electrons leave from the activated carbon are considered as positively charged and vice versa. The anions in the electrolyte are attracted to the positively charged electrode while the cations are attracted to the negatively charged electrode. Such a distribution of these cations and anions leads to the accumulation of the charge carriers at both electrodes, hence forming the electrical double layer which thereby creates the energy storage in EDLC. This phenomenon marks the completion of the charging process. As for the discharging process, the accumulated ions will move away from the electrode as the voltage is no longer applied. The study done by Liew and co-workers suggested that the cation of IL is very hard to be attached to the electrode due to its bulky structure [96]. Thus, if the electrolyte consists of both salt and IL, the cation of salt (e.g., Li^+ , Mg^+ , H^+ and Na^+) usually dominates the charge accumulation at the surface of the negative electrode.

This ion adsorption process can be affected by the amount of applied voltage used. The higher applied voltage can contribute to the increasing number of separated cations and anions in the electrolyte which will be adsorbed at the electrode interface. However, using a charging voltage that is too high may result in many separated species, resulting in an ion blocking effect and thus increasing cell resistance. Thus, this explains the determination of the stable potential range for the EDLC cell using the LSV test. To begin with, the highest volumetric capacitance and greatest charge density are found in supercapacitors [98]. Supercapacitors have found their niche as an energy storage unit and their fast charging/discharging behavior, longer cycle life, and high specific power densities which are constantly being studied for the advancement of the device are further adding to its popularity [99]. Their performance can bridge the power density and the energy density. The charge storage mechanism in EDLCs is non-Faradaic. For example, the transfer of charge between electrode and electrolyte is based on the accumulation of charges at the electrode/electrolyte interfaces under the application of an electric potential [100].

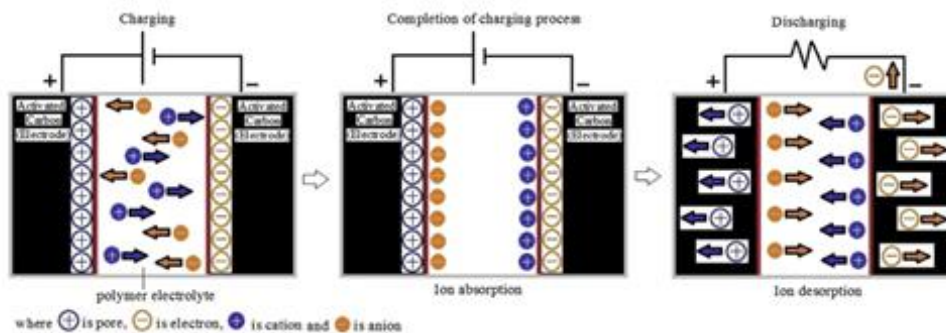


Figure 5. Charging and discharging process in EDLC.

The CD characteristics of all three anions exhibit almost linear charge-discharge curve with a small voltage drop (iR drop) at the current density of 5 A/g [94]. The ohmic resistance between electrode and electrolyte causes the initial voltage to drop in the discharge curve. The almost symmetric triangular shape of the CD curve confirms the fabricated cells' double layer capacitive nature [91]. In other work, the charge–discharge characteristics of EDLCs made using prepared polymer electrolyte and “mata kucing” fruits carbon, as well as those made with prepared polymer electrolyte and commercial activated carbon. At room temperature, the EDLCs were charged from 0 to 1.0 V at a current density of $45 \mu\text{A cm}^{-2}$ [91]. The voltage drops on discharge instantaneously. This voltage drop is caused by the EDLC's internal resistance. This loss can become dominant at large discharge currents. The efficiency of EDLCs should be more than 90% for the application of electric vehicles (EV). The internal resistance of electrochemical condensers should therefore be reduced. Resistance by electrolytes and separators (for EDLCs with liquid electrolytes), current collectors and interfluid resistance between the current collection system and the electrolytes or gel are among the contributing reasons to internal resistance.

4. CONCLUSION

PMMA-based SPEs have received a lot of attention as promising electrolytes for supercapacitors due to their excellent processing flexibility and electrode–electrolyte contact. Significant research has been conducted to improve SPEs' limited ionic conductivity and electrochemical stability at room temperature. ILs were introduced to PMMA-based SPEs to broaden the electrochemical window of PMMA. The ILs benefit from high ionic conductivity and a wide range of electrochemical media, whereas the SPEs benefit from increased flexibility and the ability to change polymer crystallinity via a crosslink or copolymerization approach. Furthermore, by utilising multiple complex PMMA-based SPEs, the supercapacitors can achieve significantly increased mechanical strength and interface stability. The development of appropriate PMMA-based SPEs is a critical issue for practical applications of high-performance supercapacitors with high safety and electrical stability.

ACKNOWLEDGEMENT

The authors would like to extend their gratitude towards the financial support from Universiti Teknologi Mara (FRGS 600-IRMI/FRGS 5/3 (116/2019) and Universiti Pertahanan Nasional Malaysia (UPNM/2018/CHEMDEF/ST/4) in the preparation of this review.

CONFLICT OF INTEREST

There are no conflicts of interest to declare.

References

1. M.S.A. Rani, M. Mohammad, M.S. Sua'it, A. Ahmad, and N.S. Mohamed, *Polymer Bulletin*, 78 (2021) 5355.
2. K. Naoi, S. Ishimoto, J.-i. Miyamoto, and W. Naoi, *Energy & Environmental Science*, 5 (2012) 9363.
3. S.B. Aziz, M.A. Brza, M.H. Hamsan, M.F.Z. Kadir, and R.T. Abdulwahid, *Polymer Bulletin*, 78 (2021) 3149.
4. A.S. Samsudin, H.M. Lai, and M.I.N. Isa, *Electrochimica Acta*, 129 (2014) 1.
5. F. Wang, X. Wu, X. Yuan, Z. Liu, Y. Zhang, L. Fu, Y. Zhu, Q. Zhou, Y. Wu, and W. Huang, *Chemical Society Reviews*, 46 (2017) 6816.
6. L. Li, C. Fu, Z. Lou, S. Chen, W. Han, K. Jiang, D. Chen, and G. Shen, *Nano Energy*, 41 (2017) 261.
7. G. Pandey, Y. Kumar, and S. Hashmi, *Indian Journal of Chemistry*, 49 (2010) 743.
8. M. Wayu, *Solids*, 2 (2021) 232.
9. P. Simon and Y. Gogotsi, *Nanoscience and technology* (2010) 320.
10. M. Lu, *Supercapacitors: materials, systems, and applications*. 2013: John Wiley & Sons.
11. N.A. Dzulkurnain, M.S.A. Rani, A. Ahmad, and N.S. Mohamed, *Ionics*, 24 (2018) 269.
12. K.H. Kamarudin, M.S.A. Rani, and M.I.N. Isa, *American-Eurasian Journal of Sustainable Agriculture*, (2015) 8.
13. M.S.A. Rani, N.A. Abdullah, M.H. Sainorudin, M. Mohammad, and S. Ibrahim, *Materials Advances*, 2 (2021) 5465.
14. O.G. Abdullah, Y.A. Salman, D.A. Tahir, G.M. Jamal, H.T. Ahmed, A.H. Mohamad, and A.K. Azawy, *Membranes*, 11 (2021) 163.
15. E. Cevik and A. Bozkurt, *Journal of Energy Chemistry*, 55 (2021) 145.
16. U. Ali, K.J.B.A. Karim, and N.A. Buang, *Polymer Reviews*, 55 (2015) 678.
17. G. Appetecchi, F. Croce, and B. Scrosati, *Electrochimica Acta*, 40 (1995) 991.
18. F. Latif, M. Aziz, N. Katun, and M.Z. Yahya, *Journal of Power Sources*, 159 (2006) 1401.
19. C.W. Liew, S. Ramesh, and R. Durairaj, *Journal of Materials Research*, 27 (2012) 2996.
20. B. Liang, S. Tang, Q. Jiang, C. Chen, X. Chen, S. Li, and X. Yan, *Electrochimica Acta*, 169 (2015) 334.
21. M.S.A. Rani, N. Mohamed, and M.I.N. Isa. *Materials Science Forum*, 846 (2016) 539.
22. Z. Osman, M.M. Ghazali, L. Othman, and K.M. Isa, *Results in physics*, 2 (2012) 1-4.
23. M.S.A. Rani, N.H. Hassan, A. Ahmad, H. Kaddami, and N.S. Mohamed, *Ionics*, 22 (2016) 1855.
24. M.A. Siti Izzati Husna, A.L. Famiza, and M.Z. Sharil Fadli. *Materials Science Forum*, 846 (2016) 528.
25. M.S.A. Rani, A. Ahmad, and N.S. Mohamed, *Ionics*, 24 (2018) 807.
26. Z.L. Xie, H.-B. Xu, A. Geßner, M.U. Kumke, M. Priebe, K.M. Fromm, and A. Taubert, *Journal of Materials Chemistry*, 22 (2012) 8110.
27. Z.L. Xie, A. Jeličić, F.-P. Wang, P. Rabu, A. Friedrich, S. Beuermann, and A. Taubert, *Journal of Materials Chemistry*, 20 (2010) 9543.
28. R. Agrawal and G. Pandey, *Journal of Physics D: Applied Physics*, 41 (2008) 223001.
29. S. Morita, *Frontiers in chemistry*, 2 (2014) 10.
30. N. Shukla and A.K. Thakur, *Ionics*, 15 (2009) 357.
31. S. Ramesh and K. Wong, *Ionics*, 15 (2009) 249.

32. T. Uma, T. Mahalingam, and U. Stimming, *Materials chemistry and physics*, 90 (2005) 245.
33. A. Ali, M. Yahya, H. Bahron, R. Subban, M. Harun, and I. Atan, *Materials Letters*, 61 (2007) 2026.
34. S. Ramesh and L.C. Wen, *Ionics*, 16 (2010) 255.
35. K. Chew and K. Tan, *Int J Electrochem Sci*, 6 (2011) 5792.
36. V.R. Jeedi, E.L. Narsaiah, M. Yalla, R. Swarnalatha, S.N. Reddy, and A.S. Chary, *SN Applied Sciences*, 2 (2020) 1.
37. K. Gohel, D. Kanchan, H.K. Machhi, S.S. Soni, and C. Maheshwaran, *Materials Research Express*, 7 (2020) 025301.
38. M. Kufian, S. Ramesh, and A. Arof, *Optical Materials*, 120 (2021) 111418.
39. S. Kang, Z. Yang, C. Yang, S. Zhao, N. Wu, F. Liu, X. Chen, and B. Shi, *Ionics*, 27 (2021) 2037.
40. C. Wheeler, K.N. West, C.L. Liotta, and C.A. Eckert, *Chemical Communications*, (2001) 887.
41. V. Le Boulaire and R. Grée, *Chemical Communications*, (2000) 2195.
42. J. Ross, W. Chen, L. Xu, and J. Xiao, *Organometallics*, 20 (2001) 138.
43. J. Howarth, P. James, and J. Dai, *Tetrahedron Letters*, 42 (2001) 7517.
44. P. Kubisa, *Progress in Polymer Science*, 34 (2009) 1333.
45. H. Olivier-Bourbigou and L. Magna, *Journal of Molecular Catalysis A: Chemical*, 182 (2002) 419.
46. I.J. Shamsudin, A. Ahmad, N.H. Hassan, and H. Kaddami, *Ionics*, 22 (2016) 841.
47. T. Sato, G. Masuda, and K. Takagi, *Electrochimica Acta*, 49 (2004) 3603.
48. S. Seki, Y. Kobayashi, H. Miyashiro, Y. Ohno, A. Usami, Y. Mita, N. Kihira, M. Watanabe, and N. Terada, *The Journal of Physical Chemistry B*, 110 (2006) 10228.
49. P. Wang, S.M. Zakeeruddin, R. Humphry-Baker, and M. Grätzel, *Chemistry of Materials*, 16 (2004) 2694.
50. A. Lewandowski and A. Świdarska, *Solid State Ionics*, 169 (2004) 21.
51. B. Singh and S. Sekhon, *Chemical physics letters*, 414 (2005) 34.
52. P. Tamilarasan and S. Ramaprabhu, *Materials Chemistry and Physics*, 148 (2014) 48.
53. W. Zhai, H.-j. Zhu, L. Wang, X.-m. Liu, and H. Yang, *Electrochimica Acta*, 133 (2014) 623.
54. L. Li, F. Wang, J. Li, X. Yang, and J. You, *International Journal of Hydrogen Energy*, 42 (2017) 12087.
55. Y.S. Vygodskii, *Polym. Adv. Technol*, 18 (2007) 50.
56. A.-L. Pont, R. Marcilla, I. De Meatza, H. Grande, and D. Mecerreyes, *Journal of Power Sources*, 188 (2009) 558.
57. H. Ohno. *Macromolecular Symposia*. 249 (2007) 551.
58. M. Watanabe, S.-i. Yamada, and N. Ogata, *Electrochimica Acta*, 40 (1995) 2285.
59. J.S. Wilkes and M.J. Zaworotko, *Journal of the Chemical Society, Chemical Communications*, (1992) 965.
60. A. Noda and M. Watanabe, *Electrochimica Acta*, 45 (2000) 1265.
61. M.A.B.H. Susan, T. Kaneko, A. Noda, and M. Watanabe, *Journal of the American Chemical Society*, 127 (2005) 4976.
62. J. Jiang, D. Gao, Z. Li, and G. Su, *Reactive and Functional Polymers*, 66 (2006) 1141.
63. V. Koch, C. Nanjundiah, G.B. Appetecchi, and B. Scrosati, *Journal of the Electrochemical Society*, 142 (1995) L116.
64. M.A. Ab Rani, (2012) Synthesis, characterization and physical-chemical properties of room temperature ionic liquids with a variety of cations, paired with bis (trifluoromethylsulfonyl) imide anion. doctoral dissertation, Imperial College, London.
65. D. Fenton, *Polymer*, 14 (1973) 589.
66. P.V. Wright, *British Polymer Journal*, 7 (1975) 319.
67. M. Armand, J. Chabagno, and M. Duclot, *Eds. Vashishta, P., Mundy, JN & Shenoy, G. K, North*

- Holland, Amsterdam, 52 (1979).
68. M.S.A. Rani, M.H. Sainorudin, N. Asim, and M. Mohammad, *International Journal of Electrochemical Science*, 15 (2020) 11833.
 69. F.G. Torres, J. Arroyo, R. Alvarez, S. Rodriguez, O. Troncoso, and D. López, *Materials Chemistry and Physics*, 223 (2019) 659.
 70. N.A. Rahman, S.A. Hanifah, N.N. Mobarak, A. Ahmad, N.A. Ludin, F. Bella, and M.S. Su'ait, *Polymer*, (2021) 124092.
 71. M.I.N. Isa, M.H. Sohaimy, and N.H. Ahmad, *International Journal of Hydrogen Energy*, 46 (2021) 8030.
 72. B. Sun, J. Mindemark, K. Edström, and D. Brandell, *Solid State Ionics*, 262 (2014) 738.
 73. M.S.A. Rani, S. Rudhzhiah, A. Ahmad, and N.S. Mohamed, *Polymers*, 6 (2014) 2371.
 74. M.L. Seol, I. Nam, E. Sadatian, N. Dutta, J.W. Han, and M. Meyyappan, *Materials*, 14 (2021) 316.
 75. D. Shriver, B. Papke, M.A. Ratner, R. Dupon, T. Wong, and M. Brodwin, *Solid State Ionics*, 5 (1981) 83.
 76. R. Younesi, G.M. Veith, P. Johansson, K. Edström, and T. Vegge, *Energy & Environmental Science*, 8 (2015) 1905.
 77. C. Zhong, Y. Deng, W. Hu, J. Qiao, L. Zhang, and J. Zhang, *Chemical Society Reviews*, 44 (2015) 7484.
 78. L. Staaf, P. Lundgren, and P. Enoksson, *Nano Energy*, 9 (2014) 128.
 79. Z. Ji, N. Li, M. Xie, X. Shen, W. Dai, K. Liu, K. Xu, and G. Zhu, *Electrochimica Acta*, 334 (2020) 135632.
 80. C.W. Liew, S. Ramesh, and A.K. Arof, *Materials & Design*, 92 (2016) 829.
 81. X. Lu, M. Yu, G. Wang, Y. Tong, and Y. Li, *Energy & Environmental Science*, 7 (2014) 2160.
 82. S. Asmara, M. Kufian, S.R. Majid, and A.K. Arof, *Electrochimica acta*, 57 (2011) 91.
 83. M.S.A. Rani, N.S. Isa, M.H. Sainorudin, N.A. Abdullah, M. Mohammad, N. Asim, H. Razali, and M.A. Ibrahim, *International Journal of Electrochemical Science*, 16 (2021) 210354.
 84. V.F. Lvovich, *Impedance spectroscopy: applications to electrochemical and dielectric phenomena*. 2012: John Wiley & Sons.
 85. S.Z.Z. Abidin, M.Z.A. Yahya, O.H. Hassan, and A.M.M. Ali, *Ionics*, 20 (2014) 1671.
 86. M.S.A. Rani, N.S. Mohamed, and M.I.N. Isa, *International Journal of Polymer Analysis and Characterization*, 20 (2015) 491.
 87. S.K. Deraman, N.S. Mohamed, and R.H.Y. Subban, *Sains Malaysiana*, 43 (2014) 877.
 88. M. Musiani, M.E. Orazem, N. Pébère, B. Tribollet, and V. Vivier, *Journal of the Electrochemical Society*, 158 (2011) C424.
 89. Y.S. Lim, H.A. Jung, and H. Hwang, *Energies*, 11 (2018) 2559.
 90. M.S.A. Rani, N.A. Dzulkurnain, A. Ahmad, and N.S. Mohamed, *International Journal of Polymer Analysis and Characterization*, 20 (2015) 250.
 91. A.K. Arof, M.Z. Kufian, M.F. Syukur, M.F. Aziz, A.E. Abdelrahman, and S.R. Majid, *Electrochimica acta*, 74 (2012) 39.
 92. A.K. Arof, S. Amirudin, S.Z. Yusof, and I.M. Noor, *Physical Chemistry Chemical Physics*, 16 (2014) 1856.
 93. D. Xuan, J. Liu, D. Wang, Z. Lu, Q. Liu, Y. Liu, S. Li, and Z. Zheng, *Energy & Fuels*, 35 (2020) 796.
 94. P. Shabeeba, M.S. Thayyil, M. Pillai, and K. Thasneema, *Journal of Molecular Liquids*, 294 (2019) 111671.
 95. C.P. Tien, W.J. Liang, P.L. Kuo, and H.S. Teng, *Electrochimica acta*, 53 (2008) 4505.
 96. C.W. Liew, S. Ramesh, and A.K. Arof, *International Journal of Hydrogen Energy*, 39 (2014) 2953.
 97. F.E. Amitha, A.L.M. Reddy, and S. Ramaprabhu, *Journal of Nanoparticle Research*, 11 (2009)

725.

98. S.B. Aziz, M.A. Brza, K. Mishra, M.H. Hamsan, W.O. Karim, R.M. Abdullah, M.F.Z. Kadir, and R.T. Abdulwahid, *Journal of Materials Research and Technology*, 9 (2020) 1137.
99. J.K. Chauhan, M. Kumar, M. Yadav, T. Tiwari, and N. Srivastava, *Ionics*, 23 (2017) 2943.
100. S.B. Aziz, M.H. Hamsan, M.A. Brza, M.F.Z. Kadir, R.T. Abdulwahid, H.O. Ghareeb, and H. Woo, *Results in Physics*, 15 (2019) 102584.

© 2022 The Authors. Published by ESG (www.electrochemsci.org). This article is an open access article distributed under the terms and conditions of the Creative Commons Attribution license (<http://creativecommons.org/licenses/by/4.0/>).